Mechanism of synchronization in a random dynamical system

Dong-Uk Hwang,[1,2,*] Inbo Kim,[1,2,†] Sunghwan Rim,[1,‡] Chil-Min Kim,[1,§] and Young-Jai Park[2,‖]

[1]*National Creative Research Initiative Center for Controlling Optical Chaos, Department of Physics, Paichai University, Seogu, Daejeon 302-735, Korea*

[2]*Department of Physics and Basic Science Research Institute, Sogang University, Seoul 100-611, Korea*

(Received 16 April 2001; published 29 August 2001)

The mechanism of synchronization in the random Zaslavsky map is investigated. From the error dynamics of two particles, the structure of phase space was analyzed, and a transcritical bifurcation between a saddle and a stable fixed point was found. We have verified the structure of on-off intermittency in terms of a biased random walk. Furthermore, for the generalized case of the ensemble of particles, *a modified definition* of the size of a snapshot attractor was exploited to establish the link with a random walk. As a result, the structure of on-off intermittency in the ensemble of particles was explicitly revealed near the transition.

DOI: 10.1103/PhysRevE.64.036219 PACS number(s): 05.45.Xt, 05.40.−a

I. INTRODUCTION

Yu, Ott, and Chen (YOC) studied a transition to chaos for a random dynamical system with the random Zaslavsky (RZ) map which describes the motion of particles floating on the surface of a fluid whose flow velocity has complicated time dependence [1,2]; the state of the system is being sampled at discrete times. It was shown that variation of a parameter causes a transition from a situation where an initial cloud of particles is eventually distributed on a fractal to a situation where the particles eventually clump at a single point, whose location moves randomly in all time. In both situations the random motion persists permanently, so the concept of attractor is inappropriate. Hence, after transient times had elapsed, they took a snapshot of the particle distribution on the fluid surface and called it *a snapshot attractor* [1,3]. They observed that the long-time particle distribution that evolves from an initial smooth distribution exhibits an ''extreme form of temporally intermittent bursting'' on the chaotic side near the transition.

After YOC's work, a type of intermittent behavior known as on-off intermittency has been reported by Platt, Speigel, and Tresser [4]. On-off intermittency refers to the situation where some dynamical variables exhibit two distinct states in their course of time evolution. One is the ''off'' state, where the variable remain approximately a constant and the other is the ''on'' state, where the variable temporarily burst out of the off state. It has long been thought that the intermittent behavior in YOC's work belongs to ''on-off intermittency'' [5–13]. However, there has been some confusion about this because YOC did not investigate the RZ map from the perspective of on-off intermittency. Indeed, in a Letter [1] and a subsequent review paper [2], they analyzed the RZ map by studying the largest Lyapunov exponent, the size of the snapshot attractor, and the simple one-dimensional contraction-expansion random map model to understand the intermittent transition behavior. But the essential geometrical structure related to the mechanism of on-off intermittency is absent in their analysis. Besides Heagy, Platt, and Hammel (HPH) commented that the snapshot attractor can undergo a form of intermittent behavior that is similar to on-off intermittency, but the size distribution of the snapshot attractor computed by YOC is quite different from the laminar phase distribution they obtained in their random walk model [14].

Meanwhile, Yang and Ding (YD) have studied a noise-driven uncoupled map lattice as a spatially extended system [15,16]. As a special case, they considered a map lattice where logistic map is located at each site uncoupled with its neighbors and each map driven by a common random variable, which is regarded as a homogeneous background. In their work, a similar transition which comes from the instability of the synchronous motion of the ensemble was found. However, on-off intermittency of the size evolution of the snapshot attractor was proposed merely on the ground of laminar distribution obtained from numerical calculations since YD were unable to map the size evolution of the snapshot attractor into a random walk. In this respect, their study was incomplete.

Recently synchronization in a pair of nonlinear systems subjected to the common noise is revisited [6,17–19]. Gade and Basu showed that this synchronization phenomena is indeed physical in certain cases, and for synchronization of those system the randomness is not vital [19]. Moreover, we have shown that, in this kind of synchronization, the distribution of the random variable is vital and there exists on-off intermittency in the boundary of synchronization region [6]. Also the intermittent behavior of the size of snapshot attractor was discussed briefly. Note that synchronization of random dynamical systems has same meaning of the chaotic transition in YOC's work. This notion of sychronization is

*Electronic address: zzamong@physics3.sogang.ac.kr
†Electronic address: ibkim@physics3.sogang.ac.kr
‡Electronic address: rim@phys.paichai.ac.kr
§Electronic address: chmkim@mail.paichai.ac.kr
‖Electronic address: yjpark@ccs.sogang.ac.kr

 ©2001 The American Physical Society

analogous to the synchronization scheme[1] proposed by Pecora and Carrol, if we assume that the random variable is realized by a system as a drive system and random dynamical systems are regarded as response systems [20].

In this paper, we explicitly show that the size evolution of the snapshot attractor really has the structure of on-off intermittency contrary to the HPH's comment. In Sec. II, we briefly recapitulate the properties of the RZ map, and in Sec. III the mechanism of synchronization of two particles will be revealed by using the error dynamics. In Sec. IV, we introduce modified definition of the size of the snapshot attractor for the case of ensemble of particles and explicitly show that this modification leads to the structure of on-off intermittency. Finally we present summary and brief discussion in Sec. V.

II. PROPERTIES OF THE RANDOM ZASLAVSKY MAP

A generic *D*-dimensional random map can be described as

$$\mathbf{r}_{n+1}=\mathbf{F}_{\xi_n}(\mathbf{r}_n), \tag{1}$$

where $\mathbf{r}_n \in \mathbb{R}^D$ is column state vector and ξ_n is a random variable. So the map $\mathbf{F}_{\xi_n}$ is chosen randomly at each iteration according to some rule generating ξ_n. As it was introduced in [1,2], the RZ map describes a particle floating on an incompressible fluid. There is constant divergence transverse to the surface, and this divergence leads to contraction on the surface. And there exists vortical flow with complicated time dependence. $\mathbf{r}_n=(x_n,y_n)^{\mathsf{T}}$ (the superscript "T" means transpose operation) describes the position of a particle on the surface at $t=nT$, where T is a constant sampling time. $\mathbf{F}_{\xi_n}$ is given by

$$\begin{aligned} x_{n+1}&=x_n+f(\alpha)y_n \mod 2\pi, \\ y_{n+1}&=g(\alpha)y_n+k\sin(x_{n+1}+\xi_n), \end{aligned} \tag{2}$$

where $f(\alpha)=(1-e^{-\alpha})/\alpha$, $g(\alpha)=e^{-\alpha}$, and k and α are control parameters. In specific, α gives rate of constant contraction of surface, k stands for the parameter of vortical flow, x is angle variable, and y is radial variable. On the other hand, random variable ξ_n gives complicated time dependence of vortical flow, which represents fluid instabilities at low Reynolds numbers. When ξ_n is absent, Eq. (2) is often called the Zaslavsky map [21]. If we consider a strip $|y|<K_0$ where $K_0>k(1-e^{-\alpha})^{-1}$, one iteration maps this strip into a narrow band $|y|<K_1<K_0$. Thus long-term behavior is confined to $|y|<k(1-e^{-\alpha})^{-1}$. Note that the Jacobian determinent of the map is $g(\alpha)=e^{-\alpha}$. Therefore, the map is contracting by the factor $g(\alpha)$ after each iteration. In this paper, we will restrict our interest to the case of $k=0.5$ as studied by YOC. Given a uniform distribution of the ensemble of particles on the surface (two dimensions), we can find the fractal distribution of particles for $\alpha<\alpha_c\simeq 0.31$ after several iterations. When we increase α close to α_c, snapshots show almost one-dimensional fractal structure (very thin line structure). And for the case of $\alpha>\alpha_c$, the snapshot collapses to a point (zero dimension), and particles move synchronously as if they were a single particle.

[1]The scheme is based on the fact that certain chaotic systems possess a self-synchronization property. A chaotic system is self-synchronizing if it can be decomposed into subsystems: a drive subsystem and a stable response subsystem that synchronize when coupled with a common drive signal.

III. SYNCHRONIZATION OF TWO PARTICLES

From now on, we will consider particles which satisfy Eq. (2). Because ξ_n is describing the geometry of vortical flow at $t=nT$ and particles are sprinkled on the surface, they have different initial conditions but feel common random driving ξ_n. To investigate the synchronization of particles, we will begin to study the dynamical behavior of two particles rather than the motion of whole ensemble of particles.

Let us consider a replica $\mathbf{r}'_n=(x'_n,y'_n)^{\mathsf{T}}$ which obeys the Eq. (2) as does $\mathbf{r}_n$. To show the mechanism of synchronization, we consider the error dynamics (ED) of this system, $\mathbf{e}_n=(u_n,v_n)^{\mathsf{T}}=\mathbf{r}'_n-\mathbf{r}_n$, which is the difference of two arbitrarily chosen particle's positions. Then, the whole system $\mathbf{z}_n=(x_n,y_n,u_n,v_n)^{\mathsf{T}}$ can be described by

$$\begin{aligned} \mathbf{r}_{n+1}&=\mathbf{F}_{\xi_n}(\mathbf{r}_n), \\ \mathbf{e}_{n+1}&=\mathbf{G}_{\phi_n}(\mathbf{e}_n), \end{aligned} \tag{3}$$

where $\mathbf{G}_{\phi_n}$ is given by

$$\begin{aligned} u_{n+1}&=u_n+f(\alpha)v_n \ \overline{\mathrm{mod}}\ 2\pi, \\ v_{n+1}&=g(\alpha)v_n+2k\cos\left(\phi_n+\frac{u_{n+1}}{2}\right)\sin\left(\frac{u_{n+1}}{2}\right) \end{aligned} \tag{4}$$

with $[A \ \overline{\mathrm{mod}}\ B]\equiv(A+B/2 \bmod B)-B/2$ and $\phi_n\equiv x_{n+1}+\xi_n$. Here, we have applied the mod operation according to the translational symmetry of u_n in trigonometric functions in Eq. (4). Note that the ED is driven by ϕ_n, which is the sum of x_{n+1} from $\mathbf{F}_{\xi_n}(\mathbf{r}_n)$ and random variable ξ_n. Therefore ϕ_n is not affected by the evolution of $\mathbf{e}_n$; hence, transformed systems have a so-called skew-product structure mathematically [4]. Because the trajectory near the hyperplane $\mathbf{e}=0$ is governed by ϕ_n, we will study properties of the ED regarding the random dynamical variable ϕ_n as a system parameter ϕ which is constant during the evolution, before considering the whole four-dimensional system.

A. Error dynamics of two particles

We will investigate the local and global bifurcation structure by finding the fixed points of $\mathbf{G}_\phi$ and its phase portrait in order to reveal the underlying structure of the ED. When we impose the conditions $u_{n+1}=u_n$ and $v_{n+1}=v_n$ on $\mathbf{G}_\phi$, $v_n f(\alpha)$ should be an integer multiple of 2π. If $v_n=0$,

$$\cos\left(\phi+\frac{u_n}{2}\right)\sin\left(\frac{u_n}{2}\right)=0. \tag{5}$$

Then, there are two fixed points

$$\mathbf{e}^* = \begin{pmatrix} u^* \\ v^* \end{pmatrix} = \begin{pmatrix} 0 \\ 0 \end{pmatrix},$$

$$\mathbf{e}^0 = \begin{pmatrix} u^0 \\ v^0 \end{pmatrix} = \begin{cases} \begin{pmatrix} \pi - 2\phi \\ 0 \end{pmatrix} & \text{for} \quad 0 \leqq \phi < \pi, \\ \begin{pmatrix} 3\pi - 2\phi \\ 0 \end{pmatrix} & \text{for} \quad \pi \leqq \phi < 2\pi. \end{cases} \tag{6}$$

When $v_n f(\alpha)$ equals $\pm 2\pi, \pm 4\pi, \ldots$, there is no additional fixed points near the transition point α_c [22]. The $\mathbf{e}_{n+1}$ near the fixed point $\mathbf{e}^*$ is written as

$$\mathbf{e}_{n+1} - \mathbf{e}^* = \mathbf{J}^*(\phi)(\mathbf{e}_n - \mathbf{e}^*) + \cdots, \tag{7}$$

where $\mathbf{J}^*(\phi) = (\partial \mathbf{G}_\phi / \partial \mathbf{e})|_{\mathbf{e}^*}$ is the Jacobian matrix evaluated at $\mathbf{e}^*$. The two eigenvalues λ_+^*, λ_-^* and the corresponding eigenvectors $\mathbf{e}_+$, $\mathbf{e}_-$ can be obtained by solving the eigenvalue problem of the matrix $\mathbf{J}^*(\phi)$. Pairs of eigenvalues give a behavior along the eigendirection of $\mathbf{e}_\pm$, and characterize the stability of $\mathbf{e}^*$ [23]. From Eq. (4), the Jacobian matrix is given by

$$\mathbf{J}^*(\phi) = \begin{pmatrix} 1 & f(\alpha) \\ k\cos\phi & g(\alpha) + k f(\alpha)\cos\phi \end{pmatrix} \tag{8}$$

and its eigenvalues are

$$\lambda_\pm^* = \frac{1}{2}\{1 + g(\alpha) + k f(\alpha)\cos\phi \pm \sqrt{(1 + g(\alpha) + k f(\alpha)\cos\phi)^2 - 4g(\alpha)}\}. \tag{9}$$

Note that λ_+^* becomes unity for $\phi = \pi/2$ or $3\pi/2$ irrespective of α and k. In Fig. 1(b) the logarithmic of $|\lambda_\pm^*|$ is plotted as a function of ϕ for $\alpha = 0.3$ and $k = 0.5$. We will use logarithmic of eigenvalues as a measure of the stability of a fixed point. Stability along the eigendirection $\mathbf{e}_+$ changes at $\phi = \pi/2$ and $\phi = 3\pi/2$. For $\phi < \pi/2$ or $\phi > 3\pi/2$, the fixed point $\mathbf{e}^*$ becomes a saddle point, at which the trajectory is attracted along the $\mathbf{e}_-$ eigendirection and repelled along the $\mathbf{e}_+$ eigendirection, since $\ln|\lambda_+^*| > 0$, $\ln|\lambda_-^*| < 0$, and $\lambda_\pm^*$ is real. For $\pi/2 < \phi < 3\pi/2$ and $\ln|\lambda_+^*| < 0$, the region of ϕ is divided into two cases. The first case is when logarithmic of the two eigenvalues are negative and different. In this region, $\mathbf{e}^*$ becomes a stable node, which makes trajectories attracted along $\mathbf{e}_+$ to the fixed point, because $\ln|\lambda_-^*| < \ln|\lambda_+^*| < 0$. For the other case, when $\ln|\lambda_+^*| = \ln|\lambda_-^*| < 0$, the two eigenvalues are a complex-conjugated pair whose absolute values are less than 1. Therefore, $\mathbf{e}^*$ becomes a stable spiral (stable foci) and the trajectory will be attracted to $\mathbf{e}^*$ rotating around the fixed point.

Similarly for the other fixed point $\mathbf{e}^0$, the Jacobian matrix is

$$\mathbf{J}^0(\phi) = \begin{pmatrix} 1 & f(\alpha) \\ -k\cos\phi & g(\alpha) - k f(\alpha)\cos\phi \end{pmatrix}, \tag{10}$$

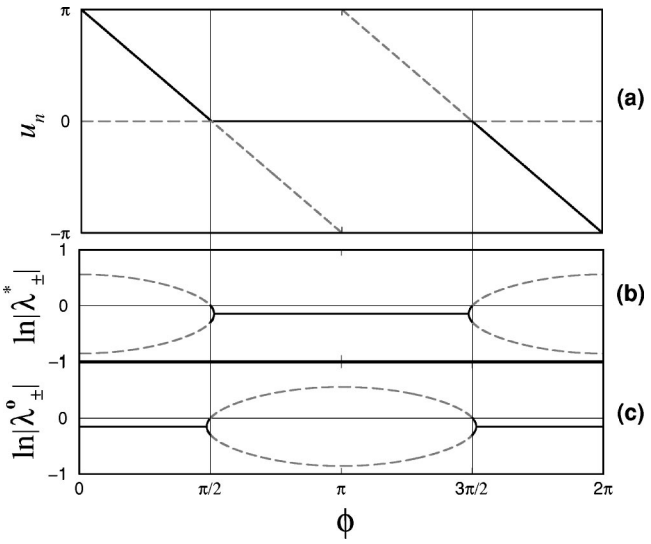

FIG. 1. (a) Bifurcation diagram of the ED. In this figure v_n is omitted because the fixed point is always 0. The horizontal axis is ϕ and its value is the same as in (b) and (c). In the diagram, solid and dashed lines stand for stable and unstable fixed points, respectively. (b) and (c) show the logarithm of the eigenvalues $(\lambda_\pm^*, \lambda_\pm^0)$ of the Jacobian matrix at $\mathbf{e}^*$ and $\mathbf{e}^0$, respectively. Vertical lines at $\phi = \pi/2, 3\pi/2$ stand for transition points of fixed points where $\ln|\lambda_+^*|$ and $\ln|\lambda_+^0|$ become 0.

and its eigenvalues are

$$\lambda_\pm^0 = \frac{1}{2}\{1 + g(\alpha) - k f(\alpha)\cos\phi \pm \sqrt{(1 + g(\alpha) - k f(\alpha)\cos\phi)^2 - 4g(\alpha)}\}. \tag{11}$$

As in the above case of $\mathbf{e}^*$, in Fig. 1(c), $\ln|\lambda_+^0|$ is zero at $\phi = \pi/2$, $3\pi/2$ irrespective of α and k. However, the situation of stability is reversed. As shown in Figs. 1(b) and 1(c), $\mathbf{e}^*$ becomes stable spiral or node (saddle) and $\mathbf{e}^0$ becomes saddle (stable spiral or node) at $\pi/2 < \phi < 3\pi/2$ $(0 < \phi < \pi/2$ or $3\pi/2 < \phi < 2\pi)$. As a result Fig. 1(a) shows a corresponding bifurcation diagram and $\mathbf{e}^*$ and $\mathbf{e}^0$ exchange stability through transcritical bifurcation at $\phi = \pi/2$ and $3\pi/2$, respectively. Note that $\mathbf{e}^*$ is constant but changes its stability with the variation of ϕ.

For some value of ϕ close to $\pi/2$ or $3\pi/2$, an attracting closed orbit and a basin boundary between the stable fixed point and the closed orbit were found in the phase portrait. Indeed, we have obtained a homoclinic bifurcation which can be found in a dissipative pendulum with constant torque [24]. In our analysis, however, we have recognized that the existence of a basin boundary as a result of global bifurcation does not affect our present results.

B. Synchronization and on-off intermittency

Our main interest in this section is the mechanism of the synchronization of two particles. Therefore, we will return to Eq. (3), where ϕ_n changes for every iteration, and consider the stability of synchronized states based on the study of the previous section. The synchronized state corresponds to $\mathbf{e}^*$

in $\mathbf{G}_{\phi_n}$. Because $\mathbf{e}^*=(0,0)$ is a fixed point of $\mathbf{G}_{\phi_n}$, the trajectory starting from $\mathbf{z}_0=(\mathbf{r}_0,\mathbf{e}^*)$ belongs to a class of a particular solution labeled by $(\mathbf{r}_0,\mathbf{e}^*)$ where $\mathbf{r}_0$ is an arbitrary chosen vector. This class of trajectories constitutes a two-dimensional invariant subset $\mathcal{M}$ embedded in the whole four-dimensional phase space. Because Eq. (3) contains the random variable ϕ_n, it will fill the whole hyperplane satisfying $\mathbf{e}=\mathbf{e}^*$ and $\mathcal{M}$ will be identical to the hyperplane. We say a subspace is *invariant* if a trajectory starting in the subspace always remains in the same subspace.

Let us consider a situation where a trajectory, which is initially located outside $\mathcal{M}$, and $\mathbf{z}_n$ happens to be located in the vicinity of $\mathcal{M}$ for some n. Whether $\mathbf{z}_{n+1}$ will be attracted or repelled from $\mathcal{M}$ is determined by the Jacobian matrix of subsystem $\mathbf{G}_{\phi_n}$ at $\mathbf{e}^*$ given by Eq. (7). Equation (7) can be mapped onto a random walk when we take the logarithm of the absolute value on each side of the equation as follows:

$$\ln|\mathbf{e}_{n+1}|=\ln|\mathbf{J}^*(\phi_n)\cdot\hat{\mathbf{e}}_n|+\ln|\mathbf{e}_n|. \tag{12}$$

Note that we have divided $\mathbf{e}_n$ into $|\mathbf{e}_n|$ and unit vector $\hat{\mathbf{e}}_n=(\cos\theta_n,\sin\theta_n)^{\mathrm{T}}$, where $\theta_n=\tan^{-1}(v_n/u_n)$. Then, one can regard $\ln|\mathbf{e}_n|$ as the nth displacement of the random walk and $\ln|\mathbf{J}^*(\phi_n)\cdot\hat{\mathbf{e}}_n|$ as its $(n+1)$th step width. The asymptotic behavior of the trajectory near $\mathcal{M}$ is determined by the average of the step width, i.e., the bias of random walk. This bias is called transverse the Lyapunov exponent $h_\perp$, which measures the global stability of $\mathcal{M}$, defined as

$$h_\perp=\int d\phi d\theta\,\rho(\phi,\theta)\ln|\mathbf{J}^*(\phi)\cdot\hat{\mathbf{e}}(\theta)|, \tag{13}$$

where $\rho(\phi,\theta)$ is probability distribution of ϕ and θ.

If $h_\perp<0$—i.e., the average of the step width is negative—the displacement of the random walk will decrease in time, and $|\mathbf{e}_n|$ will approach zero in proportion to $e^{nh_\perp}$. Therefore $\mathcal{M}$ is transeversly stable, and the whole trajectories, which initially start from outside of $\mathcal{M}$, will be attracted to $\mathcal{M}$ asymptotically. If $h_\perp>0$, the small distance between the trajectory and $\mathcal{M}$ will increase exponentially and at last will be affected by nonlinear term, which will reinject the trajectory to the neighborhood of $\mathcal{M}$. In this case $\mathcal{M}$ is called transeversly unstable. The transition from the former case to latter one according to the variation of system paramter has been investigated by others and is called ''blowout'' bifurcation [25–27].

Practically we can calculate $h_\perp$ as follows:

$$\begin{aligned} e^{nh_\perp}&=\lim_{n\to\infty}\sqrt{\frac{u_n^2+v_n^2}{\sqrt{u_0^2+v_0^2}}}\\ &=\lim_{n\to\infty}|\mathbf{J}^*(\phi_n)\mathbf{J}^*(\phi_{n-1})\cdots\mathbf{J}^*(\phi_0)\cdot\hat{\mathbf{e}}_0|\\ \to h_\perp&=\lim_{n\to\infty}\frac{1}{n}\sum_i\ln|\mathbf{J}^*(\phi_i)\cdot\hat{\mathbf{e}}_i|. \end{aligned} \tag{14}$$

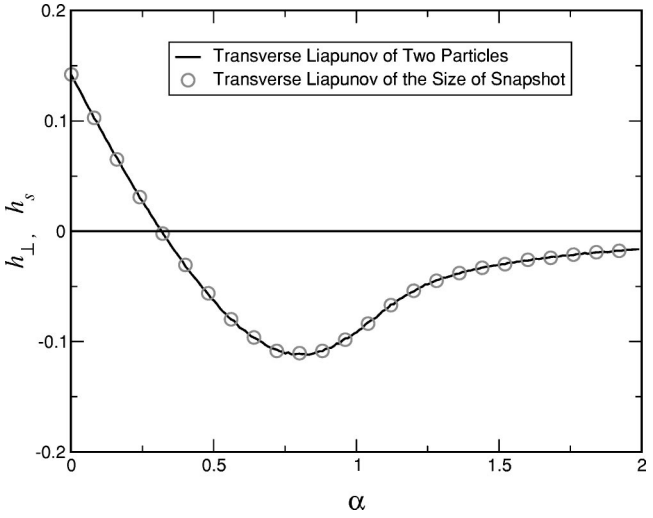

FIG. 2. $h_\perp$(solid line) and h_s(circle) vs α when $k=0.5$.

$h_\perp$ vs α graph is shown in the Fig. 2 which coincides with previous work [1,2].

It is also known that when $h_\perp$ is slightly positive, some dynamical variables of the system can exhibit an extreme type of temporal intermittent bursting behavior: on-off intermittency [14,28]. The essential ingredients of on-off intermittency are that (a) a hyperplane should contain an invariant subset and (b) the trajectory near the hyperplane shows additive random walk in the logarithmic domain depending on the local stability of the hyperplane along the transverse direction of $\mathcal{M}$ [7,28]. The trajectory in the large negative value in the logarithmic domain will be shown approximately as a constant in real scale, and corresponds to the ''off'' state. In the other case a positive or small negative value in the logarithmic domain corresponds the to ''on'' state. In the pairs of particles, we have shown that $\mathcal{M}$ is the hyperplane containing an invariant subset, and $\ln|\mathbf{e}_n|$ exhibits random walk near $\mathcal{M}$ according to the the stability of $\mathbf{J}^*$. Therefore we can conclude that there exists on-off intermittency. On the other hand, according to a result based on the study of a random walk, it is known that the probability of laminar length (L) is proportional to $L^{-3/2}e^{-L/L_s}$, where L_s is the length at which the systematic drift due to the bias and the diffusion spread of random variable without bias become comparable [5,7,14]. Figure 3 shows characteristic scaling of on-off intermittency which $P(L)$ scales as $L^{-3/2}$.

In this section, we have shown the mechanism in the synchronization of two particles using skew-product structure and a stability analysis of $\mathcal{M}$ and verified the structure of on-off intermittency.

IV. SYNCHRONIZATION OF THE ENSEMBLE OF *N* PARTICLES

In this section, we will study the behavior of an ensemble of N particles. As described in the previous section, on-off

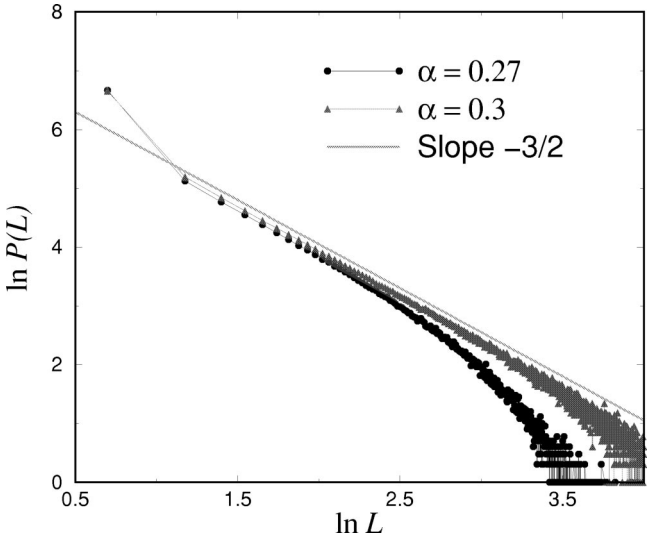

FIG. 3. Laminar distribution for two particles. The horizontal axis is the length of laminar in a logarithmic scale. The vertical axis is the logarithm of the probability of the laminar length in arbitrary units. The solid circle means the probability for $\alpha=0.27$ and solid triangle for $\alpha=0.3$. The gray straight line has a $-3/2$ slope. The case of $\alpha=0.27$ show an exponential shoulder which is typically shown in on-off intermittency models.

intermittency can be characterized by a biased random walk. To establish the link with a random walk with the size evolution of the snapshot attractor, let us consider the relation between the ED and the size of the snapshot attractor. YOC considered the size of the snapshot attractor S_n as the rms (root mean square) value of distance from the center of mass of the ensemble as

$$S_n=\sqrt{\frac{1}{N}\sum_{i=1}^{N}(y_n^i-\overline{y_n})^2}, \tag{15}$$

where y_n^i are coordinates of the ith particle ($i=1,2,\ldots,N$) and $\overline{y_n}=N^{-1}\Sigma_i y_n^i$. However, $\overline{y_n}$ is not so good a choice to establish the random walk relation between S_n and S_{n-1}. Since $\overline{y_n}$ is defined as the average of y_n^i and S_n^2 can be expressed by $\overline{y_n}$ and $(\overline{y_n})^2$, it is difficult to obtain S_{n-1} from the definition of S_n in the limit of $S_n\to 0$. In order to use the result from the previous section, we consider the modified measure $\tilde{S}_n$ which is the average length not from the center of the ensemble $\overline{y_n}$ but from an arbitrarily chosen reference particle position y_n^r in the ensemble. Our modified measure is defined as

$$\tilde{S}_n=\sqrt{\frac{1}{N}\sum_{i}(y_n^i-y_n^r)^2}=\sqrt{\frac{1}{N}\sum_{i}(v_n^i)^2}, \tag{16}$$

which is the rms distance in the y direction, where $v_n^i=y_n^i-y_n^r$. The behavior of S_n and $\tilde{S}_n$ can be seen in Fig. 4 for the case $N=1000$, $\alpha=0.3$, and $k=0.5$. Figure 4(b) shows that the amplitudes are slightly different, but bursting and laminar behaviors coincide. Moreover, as shown in Fig. 4(a), as S_n

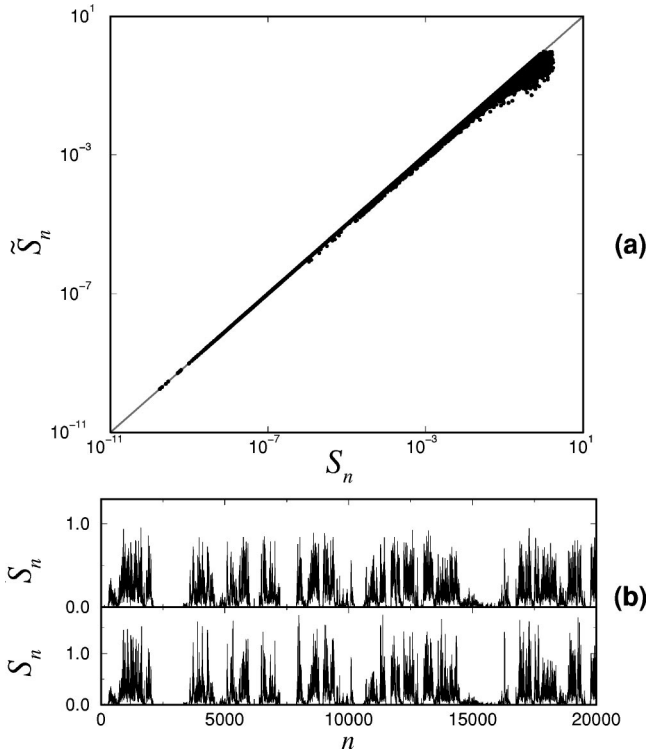

FIG. 4. (a) Horizontal and vertical axes are S_n and $\tilde{S}_n$ in the logarithmic scale, respectively. Both axes are the logarithmic scale. Solid dots are data from 1000 particles when $\alpha=0.3$ and grayed line is the diagonal line. Data close to zero lie on the diagonal line and that means S_n and $\tilde{S}_n$ become identical. (b) shows the time series of S_n and $\tilde{S}_n$ for the same period. Although amplitudes are slightly different from each other, the timings of the bursting and laminar periods coincide.

approaches 0, $\tilde{S}_n$ becomes identical to S_n. Therefore $\tilde{S}_n$ may be replaced with S_n when one investigates the size of the snapshot attractor near the synchronization transition point. Since our measure $\tilde{S}_n$ can be decomposed into the rms value of the ED variable v_n^i, the relation between $\tilde{S}_{n+1}$ and $\tilde{S}_n$ can be obtained from the relation between v_{n+1} and v_n. In the measure of $\tilde{S}_n$, the existence of the hyperplane containing the invariant set is guaranteed by the invariant hyperplane of the two-particle system—that is, the hyperplane stands for the state when all the particles move synchronously.

A. Uncoupled map lattice with homogeneous background

We analyzed the one-dimensional simple case of globally coupled logistic maps which was studied by YD [15,16]. Let us consider the system of N particles. They are located at $y_n^1,\ldots,y_n^N$, and their dynamics is described by

$$y_{n+1}^i=z_n y_n^i(1-y_n^i), \tag{17}$$

where $z_n=a\xi_n+b$ and ξ_n is a random variable uniformly distributed in the interval (0,1]. Note that this system is identical to the model studied by HPH [14] to explain on-off intermittency. When $a=1$ is fixed and b is varied, they re-

ported that the transition from the nonsynchronous state to the synchronous one is found at $b_c=2.82$, and when $b>b_c$, the size evolution of the snapshot attractor exhibits on-off intermittency. We will explain this transition behavior with our measure $\tilde{S}_n$ and the ED. If we consider the difference v_n^i between y_n^i and y_n^r such that

$$v_{n+1}^i=y_{n+1}^i-y_{n+1}^r=z_n v_n^i(1-2y_n^r-v_n^i), \tag{18}$$

then,

$$\tilde{S}_{n+1}^2=\frac{1}{N}\sum_{i=1}^{N}(v_{n+1}^i)^2=\frac{1}{N}\sum_{i=1}^{N}z_n^2(v_n^i)^2(1-2y_n^r-v_n^i)^2. \tag{19}$$

If we consider the limit $v_n^i\to 0$ and neglect higher order terms $\Sigma_i(v_n^i)^3$ and $\Sigma_i(v_n^i)^4$ near the transition region, Eq. (19) becomes $\tilde{S}_{n+1}\simeq|z_n(1-2y_n^r)|\tilde{S}_n$. Then, we have obtained the following relation by taking the logarithm on both sides:

$$\ln\tilde{S}_{n+1}=\ln|z_n(1-2y_n^r)|+\ln\tilde{S}_n. \tag{20}$$

This relation can be interpreted such that the size evolution of the snapshot attractor in the logarithmic domain is governed by the random walk with a step size $\ln|z_n(1-2y_n^r)|$. Similarly to Eq. (13) the transverse Lyapunov exponent is

$$h_\perp=\int dy\,\rho(z,y)\ln|z(1-2y)|, \tag{21}$$

where $\rho(z,y)$ is the invariant probability density. This leads to the same transition point which is calculated by YD. One should notice that the random variable is multiplied *commonly* to every particle in the summation of Eq. (19), and this leads to on-off intermittency of $\tilde{S}_n$.

B. RZ map

In the case of the RZ map, we consider the case of $v_n^i\simeq 0$. From Eq. (4),

$$\begin{aligned}v_{n+1}^i&=g(\alpha)v_n^i+2k\cos(\phi_n+u_{n+1}^i/2)\sin(u_{n+1}^i/2)\\&=g(\alpha)v_n^i+k\cos\phi_n\sin\{[\cot\theta_n^i+f(\alpha)]v_n^i\}\\&\quad-2k\sin\phi_n\sin^2\{[\cot\theta_n^i+f(\alpha)]v_n^i/2\}\\&\simeq\{g(\alpha)+k\cos\phi_n[\cot\theta_n^i+f(\alpha)]\}v_n^i+O((v_n^i)^2),\end{aligned} \tag{22}$$

where $\cot\theta_n^i=u_n^i/v_n^i$ and $u_{n+1}^i=[\cot\theta_n^i+f(\alpha)]v_n^i$. Therefore,

$$\begin{aligned}\tilde{S}_{n+1}^2&=\frac{1}{N}\sum_i[v_{n+1}^i]^2\\&\simeq\frac{1}{N}\sum_i\{g(\alpha)+k\cos\phi_n[\cot\theta_n^i+f(\alpha)]\}^2(v_n^i)^2\\&\quad+\frac{1}{N}\sum_i O[(v_n^i)^3].\end{aligned} \tag{23}$$

Then, Eq. (23) has a different result compard with the previous case, because the summation in Eq. (23) does not have a common driving. As a result, it seems that one could not deduce $\tilde{S}_n$ from the right side. However, we have recognized the crucial property that the value of $\cot\theta_n^i$ for all i becomes identical when $v_n^i\simeq 0$, which will be explained in detail in the following. That property means that the whole particles align in a line passing through the reference particle, because $\tan\theta_n^i$ is the slope of a line connecting position of the reference particle to that of the ith particle. In Sec. III, we have shown that **e*** becomes a saddle or a spiral for most ϕ. When **e*** is a saddle, particles are repelled along the unstable direction. However, since $|\ln|\lambda_+^*||<|\ln|\lambda_-^*||$, particles are attracted fast along $\mathbf{e}_-$ and repelled slowly along $\mathbf{e}_+$. Therefore, particles are scattered around along the unstable eigendirection after a few iteration, and become a narrow stripe along a straight line from the reference particle. When **e*** is a spiral, we have shown that the particles around **e*** rotate around the fixed point without changing the shape of distribution. Figure 5 shows the behavior of particles near **e*** for constant ϕ when **e*** is a saddle or spiral. After particles are scattered along a line, the Jacobian matrix maps the line passing through the position of the reference particle to another line passing through that of the reference particle. Therefore, we could approximate $\cot\theta_n=\cot\theta_n^1=\cot\theta_n^2=\cdots=\cot\theta_n^N$ for $\tilde{S}_n\simeq 0$.

This result is consistent with the finding of YOC that the Lyapunov dimension becomes unity on the chaotic side of the transition. This represents that the ensemble of N particles is embedded in a one-dimensional manifold. Also from the evolution of the uniformly distributed ensemble, we have found that near the fixed point all the particles are aligned in a line from the position of the reference particle as shown in Fig. 6. Therefore, we can write as follows:

$$\tilde{S}_{n+1}=|g(\alpha)+k\cos\phi_n[\cot\theta_n+f(\alpha)]|\tilde{S}_n. \tag{24}$$

By taking the logarithm on both sides, we find

$$\ln\tilde{S}_{n+1}=\ln|g(\alpha)+k\cos\phi_n[\cot\theta_n+f(\alpha)]|+\ln\tilde{S}_n. \tag{25}$$

As a result, Eq. (25) shows a random walk process in the logarithmic domain. The transition point of the size of the snapshot attractor is determined by the transverse Lyapunov exponent h_s, which is the average step size in Eq. (25), as follows:

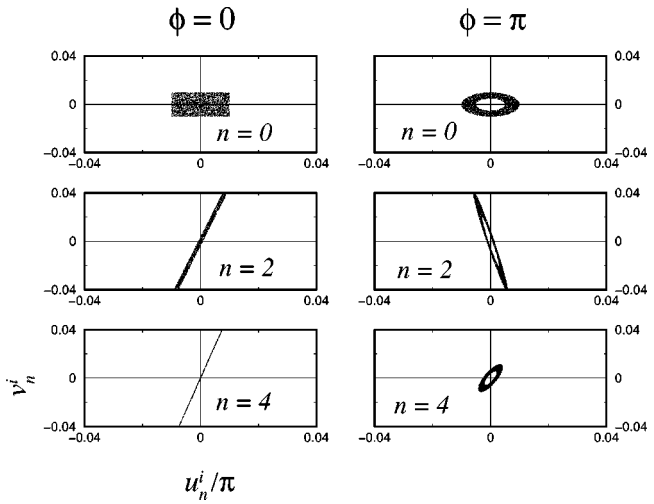

FIG. 5. Evolution of an ensemble of 5000 particles for constant ϕ when $\alpha=0.3$ and $k=0.5$. Left columns of the three graphs are initial evolution of the ensemble with $\phi=0$, where the fixed point at $\mathbf{e}^*$ is a saddle. We start with random initial points distributed within $-0.01<u_0/\pi<0.01$ and $-0.01<v_0<0.01$ uniformly in order to show the behavior near the saddle. From upper to lower graphs, the shape of the ensemble stretches along the unstable manifold as time flows. In contrast to the left ones, the right columns are that of the ensemble when $\phi=\pi$ and the fixed point is spiral. The distribution, which is initially located in a ring, rotates around the origin with contracting its area. Note that in these graphs coordinates are u_n^i and v_n^i/π, i.e., relative displacement from the reference particle.

$$h_s=\lim_{n\to\infty}\frac{1}{n}\sum_{i=1}^{n}\ln|g(\alpha)+k\cos\phi_n[\cot\theta_n+f(\alpha)]|. \quad (26)$$

In Fig. 2, the h_s, which is numerically obtained by using the original map (2), shows the same result of $h_\perp$ which is calculated in the case of two particles. In this case the invariant hyperplane is a subspace satisfying $v_n^i=0$ and $u_n^i=0$ for all i. By the hyperplane and the previous random walk relation the existence of on-off intermittency of $\tilde{S}_n$ is verified. Furthermore, in the plot of the laminar distribution of $\tilde{S}_n$, the distribution is not affected by the number of particles and shows the same scaling of the two-particle case, as depicted in Fig. 7, which shows the consistency of our results.

V. SUMMARY AND DISCUSSION

In this paper, we have considered the mechanism of synchronization in a random dynamical system. As a specific example, we have investigated the random Zaslavsky map in detail. From the ED of two particles, we have studied the bifurcation structure of the invariant manifold and found transcirtical bifurcation between the saddle and stable node. Our results are consistent with those of YOC, but are more explicit in the perspective of on-off intermittency structure. In the case of an ensemble of many particles in the random Zaslavsky map, the long-standing problem to map the size

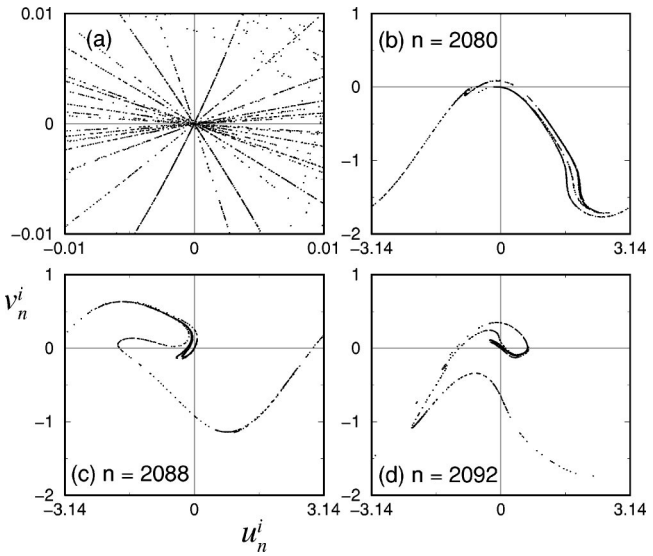

FIG. 6. Snapshot of 5000 particles when $\alpha=0.3$ and $k=0.5$. Initially, particles are distributed in the region $-0.5<u_0<0.5$ and $-0.5<v_0<0.5$. (b), (c), and (d) show a fractal distribution of particles when $n=2080$, 2088, and 2092, respectively. (a) shows a small area of the snapshot attractor for $n=2080,2081,\ldots,2099$ in the same graph. In this region particles are aligned in a line for each instant time when particles are close to the origin. Each line stands for a snapshot for a given instant time. Note that in these graphs coordinates are u_n^i and v_n^i, i.e., relative displacement from the reference particle.

evoultion of the snapshot attractor into a random walk is at last resolved by exploiting our modified definition of the size of the snapshot attractor, which is slightly different from the previously proposed one. From this success of mapping onto a random walk, we have obtained a qualitative understanding why this manifestation of intermittency has the same critical

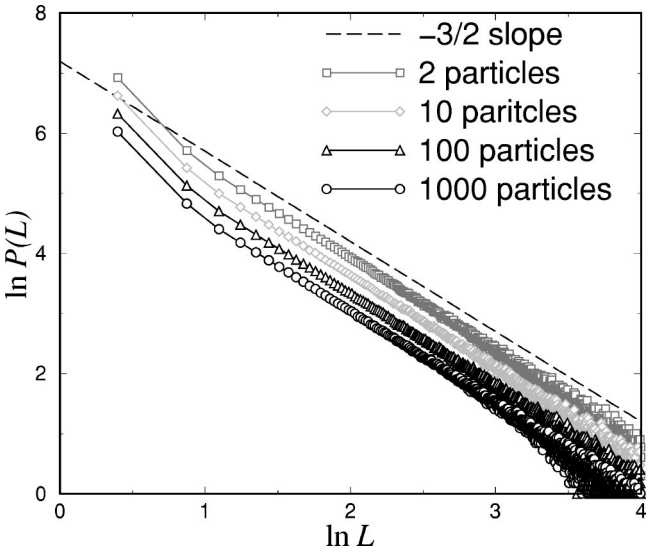

FIG. 7. Probability distribution $P(L)$ of laminar length L when $\alpha=0.3$ and $k=0.5$. We choose the threshold of an event as 10^{-4}. The unit of probability is arbitrary.

exponent, which is found from numerical simulation as that of the typical on-off intermittency. We emphasize that this mapping becomes possible when the ED variables are distributed on a line along the unstable direction of the saddle. For further investigation, it will be interesting to study other systems that seem to be difficult to map onto the form of a random walk.

ACKNOWLEDGMENTS

We thank P. Kang for valuable discussions. This work was supported by Creative Research Initiatives of the Korean Ministry of Science and Technology. Two of us (I.K. and Y.-J.P.) acknowledge support from the Ministry of Education, BK21 Project No. D-1099.

[1] L. Yu, E. Ott, and Q. Chen, Phys. Rev. Lett. **65**, 2935 (1990).
[2] L. Yu, E. Ott, and Q. Chen, Physica D **53**, 102 (1991).
[3] F.J. Romeiras, C. Grebogi, and E. Ott, Phys. Rev. A **41**, 784 (1990).
[4] N. Platt, E.A. Spiegel, and C. Tresser, Phys. Rev. Lett. **70**, 279 (1993).
[5] H.L. Yang and E.J. Ding, Phys. Rev. E **54**, 1361 (1996).
[6] S. Rim, D.-U. Hwang, I. Kim, and C.-M. Kim, Phys. Rev. Lett. **85**, 2304 (2000).
[7] M. Ding and W. Yang, Phys. Rev. E **52**, 207 (1995).
[8] Y.-C. Lai, Phys. Rev. E **53**, R4267 (1996).
[9] M. Ding and W. Yang, Phys. Rev. E **56**, 4009 (1997).
[10] Y.-C. Lai, Phys. Rev. E **54**, 321 (1996).
[11] Z. Qu, F. Xie, and G. Hu, Phys. Rev. E **53**, R1301 (1996).
[12] A. Stefański, T. Kapitaniak, J. Brindley, and V. Astakhov, Phys. Rev. E **57**, 1175 (1998).
[13] W.-H. Kye and D. Topaj, Phys. Rev. E **63**, 045202 (2001).
[14] J.F. Heagy, N. Platt, and S.M. Hammel, Phys. Rev. E **49**, 1140 (1994).
[15] H.L. Yang, and E.J. Ding, Phys. Rev. E **50**, R3295 (1994).
[16] H.L. Yang, Z.Q. Huang, and E.J. Ding, Phys. Rev. E **54**, 3531 (1996).
[17] S. Fahy and D.R. Hamman, Phys. Rev. Lett. **69**, 761 (1992).
[18] A. Maritan and J.R. Banavar, Phys. Rev. Lett. **72**, 1451 (1994).
[19] P.M. Gade and C. Basu, Phys. Lett. A **217**, 21 (1996).
[20] L.M. Pecora and T.L. Carroll, Phys. Rev. Lett. **64**, 821 (1990).
[21] G.M. Zaslavsky, Phys. Lett. **69A**, 145 (1978).
[22] Fixed points can be found analytically. When $v_n f(\alpha)=2l\pi$ for $l=\pm 1,\pm 2,\ldots$, after applying the conditions $u_{n+1}=u_n$ and $v_{n+1}=v_n$, we obtain $\sin u_n=2l\pi\alpha/k+\sin\phi$ from Eq. (4). For given l this equation has solutions when $\alpha<1/4\pi l$. When $l=\pm 1$, a soultion exists for $\alpha<1/4\pi\simeq 0.16$. However, these fixed points do not affect our analysis because 0.16 is fairly apart from the transition point α_c. When $l=\pm 2,\pm 3,\ldots$, the range of α where solutions exist becomes smaller than the range in the case of $l=\pm 1$; therefore, all the other fixed points except the case of $v_n f(\alpha)=0$ are irrelevant to our analysis.
[23] F.C. Moon, *Chaos and Fractal Dynamics: An Introduction for Applied Scientists and Engineers* (Wiley, New York, 1992).
[24] J. Guckenheimer and P. Holmes, *Nonlinear Oscillations, Dynamical Systems, and Bifurcations of Vector Fields* (Springer-Verlag, New York, 1983); see Sec. 4.7.
[25] E. Ott and J.C. Sommerer, Phys. Lett. A **188**, 39 (1994).
[26] P. Ashwin, J. Buescu, and I. Stewart, Phys. Lett. A **193**, 126 (1994).
[27] Y.C. Lai and C. Grebogi, Phys. Rev. E **52**, R3313 (1995).
[28] N. Platt, S.M. Hammel, and J.F. Heagy, Phys. Rev. Lett. **72**, 3498 (1994).